Potential energy surface of H2O on Al{111} and Rh{111} from theoretical methods

Víctor A. Ranea

Citation: J. Chem. Phys. **137**, 204702 (2012); doi: 10.1063/1.4767766
View online: http://dx.doi.org/10.1063/1.4767766
View Table of Contents: http://jcp.aip.org/resource/1/JCPSA6/v137/i20
Published by the American Institute of Physics.

Potential energy surface of H_2O on Al{111} and Rh{111} from theoretical methods

Víctor A. Ranea[a)]
CCT-La Plata-CONICET, Instituto de Investigaciones Fisicoquímicas Teóricas y Aplicadas (INIFTA), Facultad de Ciencias Exactas, Universidad Nacional de La Plata, Calle 64 y Diagonal 113, 1900 La Plata, Argentina

(Received 14 April 2012; accepted 2 November 2012; published online 29 November 2012)

The potential energy surfaces of molecular water on the Al{111} and on the Rh{111} metal surfaces have been investigated using density functional theory. Similar landscapes were found on both surfaces. In the only minimum found, the water molecule is monocoordinated to the surface via the oxygen atom (*top* configuration) with its plane nearly parallel to the surface. The maxima are around the *bridge* and *hollow* configurations and no local minima or maxima were found. Along the investigated minimum energy pathways, no strong preferential orientation of the water dipole was found, as long as the molecular plane is nearly parallel to the surface. © *2012 American Institute of Physics*. [http://dx.doi.org/10.1063/1.4767766]

I. INTRODUCTION

The interaction of water (H_2O) with surfaces has been the subject of study of numerous experimental and theoretical works due to its importance in topics of physics, chemistry, etc.[1–3] Water/metal systems have received much attention and a number of studies aimed at understanding the adsorption and diffusion of water molecules on single crystal metal surfaces have been performed.[4–19] In particular, scanning tunneling microscopy (STM) studies have been carried out in which the adsorption and diffusion of H_2O monomers and small clusters have been examined on Pd{111}.[6] However, the internal structure of the adsorbed H_2O molecules has not yet been resolved with STM. Although diffusion of adsorbates on surfaces plays an important role in a wide variety of processes, including cluster formation, surface wetting, crystal growth, corrosion, and heterogeneous catalysis, the microscopic diffusion mechanisms are not known yet, at the atomic level, for water on a metal surface. A reliable theoretical model can shed light on the details of the internal structure of the water molecules after adsorption and in the diffusion process on a metal surface.

It has been demonstrated that density functional theory (DFT) is a high-quality approach for the investigation of the adsorption and diffusion of atoms and molecules on metal surfaces.[20–23] Excellent agreement can be obtained between experimentally determined and DFT calculated diffusion barriers.[24,25]

It is often assumed that the potential energy surface for adsorbate diffusion on a homogeneous surface, can be described by a cosinelike function, where the stable configurations are at high-symmetry sites.[26] Within this frame, the energy barrier for adsorbate diffusion could be obtained by comparing adsorption energies at high-symmetry sites, but this is not always the case, as shown by Ge and King for CO diffusion on the Pt{110} surface.[22] Analysis of quasielastic helium atom scattering data of CO diffusion on Cu{100} indicate that the top configuration is the favored site and the energy barrier is attributed (without further analysis) to the energy of the bridge site in the one-dimensional potential energy surface (PES). Similar one-dimensional PES functions have also been assumed when other systems, such as CO on Ni{110}, CO on Ni{100}, Na on Cu{111}, S on Cu{111}, CO on Pt{111} and Pb on Pb{110}, have been studied with that experimental technique. These systems have been reviewed by Hofmann and Toennies.[27] Ge and King using DFT calculations have found that the detailed analysis of the one-dimensional PES of CO on Pt{110}, without assumptions, leads to a different conclusion. They found a maximum between top and bridge configurations, and that these two adsorption sites are minima in the one-dimensional PES. In the present article, the PES of H_2O on the Al{111} and on the Rh{111} metal surfaces is investigated within the DFT and the climbing image nudged elastic band (cNEB) frameworks. Questions like: How is the molecular dipole and the molecular plane of a water molecule oriented when diffusion takes place? Is the water diffusion on these surfaces a likely process? Is the water diffusion a random walk process or there are directions or paths more likely than others? have a reliable answer using DFT and cNEB methods.

In a previous article, the cluster method was used to simulate the interaction of a water molecule with the Al(111) surface.[28] The calculations were performed at the restricted open shell Hartree-Fock level using the GAMESS code. Two clusters were used to mimic the Al surface, Al_{10} and Al_{17}. The first one was made of a single ten-atom layer and the second one was made of two layers of ten and seven atoms, respectively. This approximation assumes that the adsorbate-substrate interaction is dominated by local effects. But some characteristics of the adsorption may be influenced by the size and/or shape of the cluster used in the calculations. In these two small clusters, most of the atoms do not have the same environment that they have in a surface. In a larger cluster (wider and deeper), most of the surface atoms near the

a)vranea@inifta.unlp.edu.ar.

adsorbate location are much closer to their ideal environment on the surface and also the electronic structure. The interaction between a water molecule and a metal surface would be better described by a larger cluster in which the wavefunctions of the surface atoms of the cluster, near the adsorbate, are like or similar to the wavefunctions of the surface. In the present article, periodic boundary conditions are applied and a deeper slab is used in order to mimic the interaction of a water molecule with the surface.

The adsorption of water on the Rh{111} surface was investigated previously using experimental techniques[10] and DFT.[13] In both studies the water coverage is higher than the coverage studied in this work. In those works the interaction of every adsorbed water molecule is with the surface and also with other adsorbed water molecules, whereas in the present work the main interaction of the adsorbed water molecule is with the surface. On a metal surface, at high coverage (2/3 ML[13]), the water layer is made due to a balance between the interaction among water molecules and the interaction between a water molecule and the surface. These interactions are of different nature: the interaction between a water molecule and the surface is via the water molecular orbitals ($1b_1$, mainly, and $3a_1$, as long as the molecular plane is nearly parallel to the surface plane) with the wavefunctions of the surface,[16,19] whereas the interaction among water molecules is H-bond. Similar DFT calculations[13] for 2/3 ML coverage show that the oxygen of the water molecule is at 2.54 Å from the Rh surface atom, whereas, in the present work, for 1/4 ML coverage, the water molecule is above the top surface atom at a distance of 2.33 Å. The ≈0.2 Å difference is probably due to the three H-bonds the water molecule has at 2/3 ML coverage that weakens its interaction with the surface.

In the present article, for these two surfaces (Al{111} and Rh{111}), a minimum is found for water adsorption on the *top* configuration with its plane nearly *parallel* to the surface. A *flat* and *wide* maximum is found for H_2O adsorption around the *bridge* and *hollow* configurations, for these two metal surfaces. As a consequence, the barrier for H_2O diffusion from *top* to *top* configurations is almost independent of the chosen pathway. The orientation of the molecular plane is investigated as well as the orientation of the water dipole.

II. METHODOLOGY

Calculations were performed within the density functional theory framework[29,30] as implemented in the Vienna *ab initio* simulation package[31,32] code. The Kohn-Sham equations were solved using projector augmented wave method[33,34] and a plane-wave basis set including plane waves up to 400 eV. Electron exchange and correlation energies were calculated within the generalized gradient approximation in the Perdew-Wang 91 form.[35] In order to find stable adsorption configurations, the atomic structure and the total energy were considered converged when the forces on the ions were less than 0.03 eV/Å. Periodic boundary conditions were applied. The Hessian matrix of second derivatives was determined for ground structures within the harmonic approximation by two-sided finite differences, using a displacement step of 0.01 Å. Adsorbed atoms were displaced in the calculations, and diagonalization of the dynamic matrix gave the harmonic frequencies. The cNEB method was used to calculate the minimum energy pathway (MEP) between two converged configurations[36,37] and the maximum of every MEP. Three images were used in the calculation of the MEPs between the *top* and the *bridge* or *hollow* configurations. The atomic structure and the total energy of the images in the cNEB calculations were considered converged when the forces on the ions were less than 0.03 eV/Å. The first Brillouin zone was sampled by a $(5 \times 5 \times 1)$ Γ centered Monkhorst-Pack[38] mesh, resulting in 13 k-points and only the Γ point was used in the gas phase case.

The system (aluminium or rhodium surface and the H_2O molecule) was modeled by a $p(2 \times 2)$ surface unit supercell with a depth equivalent to twelve-layers. The lattice constants of the hexagonal aluminium (rhodium) supercell were $a = 5.73$ (5.37) and $c = 28.06$ (26.35) Å.[39] Every surface was modelled by a periodic array of five-layer slabs separated by a vacuum region. A single H_2O molecule was adsorbed on one side of the slab within the supercell (coverage of $\theta = 0.25$ ML). The supercell is large enough to avoid interactions between slabs due to the periodic boundary conditions in the [111] direction. The adsorption energy, E_a, is defined relative to the H_2O molecule gas phase energy and the energy of the clean optimized surface. It is calculated as

$$E_a = E(H_2O/srf) - E(H_2O) - E(srf). \quad (1)$$

The first term of Eq. (1) is the energy of the optimized configuration of H_2O adsorbed on the clean relaxed surface. The atoms of the two external layers of the surface and the atoms of the adsorbate were allowed to relax freely. The second term of Eq. (1) is the H_2O gas phase energy. To calculate the energy of the isolated H_2O molecule, a 15 Å side cubic supercell was used and the three atoms were allowed to relax freely. The third term of Eq. (1) is the energy of the clean optimized surface. The atoms of the two external layers of the surface were allowed to relax freely.

According to Eq. (1), a negative value of E_a will indicate a stable configuration, see Table I. (The vertical axis of Figures 2–4 is labeled "Relative energy" and begins in 0 eV. The relative energy is with respect to the H_2O adsorption energy in the *top* configuration on the corresponding substrate.)

III. RESULTS AND DISCUSSION

H_2O adsorption was investigated at all four high-symmetry adsorption sites on the fcc{111} surface of Al and Rh: *top*, *bridge*, *hcp* and *fcc hollow*. Initially the molecular plane was set parallel to the surface, or perpendicular to the surface with the hydrogens away from it. The investigated sites are marked on Figure 1.

Table I shows energies and structural optimized parameters of H_2O adsorption on the Al{111} and Rh{111} surfaces. The adsorption model presented here is consistent with the common binding mechanism identified in previous works on transition and noble metal surfaces.[16,19] On both surfaces, the H_2O molecule binds most strongly to the *top* site with a calculated adsorption energy of −0.26 and −0.35 eV on Al and Rh, respectively. As a reference on the Al surface, the

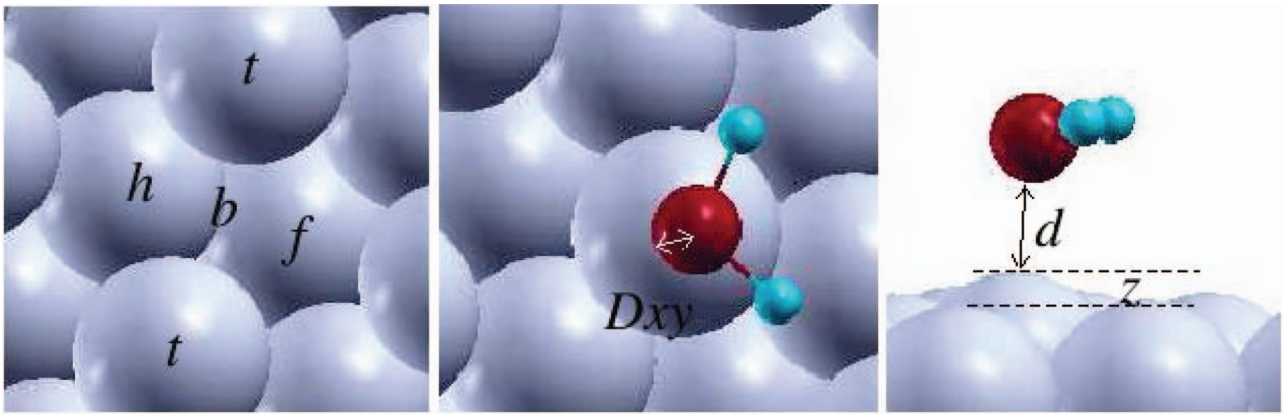

FIG. 1. (Panel on the left): Top view of the fcc{111} clean surface. The investigated high-symmetry adsorption sites are marked: *t*, *b*, *f*, and *h* are for *top*, *bridge*, *fcc hollow,* and *hcp hollow* sites, respectively. (panels at the center and on the right) Top and side views of the H_2O adsorption on *top* site on the Al and Rh{111} surfaces. The molecule is monocoordinated to the surface via its oxygen atom and shifted by D_{xy} from the exact top position in the direction of the molecular dipole. The top metal atom is pulled out of the surface by *z* after interaction with the H_2O molecule with respect to the other surface metal atoms. The O-*top* metal atom distance is denoted as *d*, also shown in Table I. Big, medium, and small spheres represent metal, oxygen, and hydrogen atoms, respectively.

adsorption energy calculated allowing the relaxation of only the water molecule, with the Al atoms kept in their bulk positions is −0.23 eV. There is no change in the adsorption energy ($E_a = -0.26$ eV) when the water molecule and only the most external layer are allowed to relax. The adsorption energy calculated on Al is below the range of 0.57 to 0.87 eV (13 kcal/mol to 20 kcal/mol) obtained using cluster calculations for different cluster sizes (Al_{10} and Al_{17}, respectively).[28] However, the adsorption energies calculated in the present work are within the range obtained for transition and noble metal surfaces using similar DFT methods.[16] The H_2O adsorption energy calculated on Rh is slightly less exothermic (0.07 eV) than the one presented in Ref. 16 using similar DFT methods. H_2O adsorption on *top* configuration is in agreement with experimental results on Pd{111}.[6] Salmeron and co-workers[6] using STM found that the water monomer spends most of the time on *top* configuration at low temperature and very low coverage on Pd.

On the studied surfaces, the plane of the molecule is nearly parallel to the surface plane, in agreement with previous similar DFT works.[16] On Al{001}, a similar result has previously been found,[17] whereas cluster approximations[28] found that the molecular plane is normal to the surface plane. In this work, no stable configuration was found with the molecular plane perpendicular to the surface.

The oxygen is laterally shifted from the exact top position by 0.19 and 0.14 Å on Al and Rh, respectively; and the top metal atom undergoes a vertical displacement of 0.23 and 0.07 Å with respect to the other surface metal atoms. The difference in the adsorption energy on *top* configuration was calculated to be less than 0.01 eV for several orientations of the molecular dipole, as long as the molecular plane is nearly parallel to the surface plane. This indicates a very low activation energy for rotation of the molecule around an axis that is perpendicular to the {111} plane and that passes through the top atom. The molecular dipole exhibits no preferential orientation, even at low temperatures, as long as the molecular plane is nearly parallel to the surface plane.

Adsorption at the *bridge* site, *fcc* and *hcp hollow* sites is less stable, with adsorption energies of −0.10, −0.10, and −0.09 eV, respectively, on the Al surface. A slightly stronger interaction was found on the Rh surface, as shown in Table I. The structure of the molecule is slightly modified from the gas phase by the presence of the substrate (Al or Rh) when the adsorption takes place regardless of the adsorption configuration. At all three sites the plane of the H_2O

TABLE I. Energies and structural optimized parameters for the H_2O molecular adsorption on the fcc{111} metal surfaces Al and Rh: adsorption energy (E_a, eV), H_2O dipole-normal to the surface tilt angle (α, °), lateral displacement of the O atom from the precise site (D_{xy}, Å), O atom-metal atom(s) vertical separation (*h*, Å), O atom-metal atom(s) distance(s) (*d*, Å) and vertical spacing between the metal atom(s) that interact directly with the H_2O molecule and the rest of the layer (*z*, Å), for every adsorption site. In the column on the right the calculated vibrational frequencies are shown for every adsorption configuration: antisymmetric stretching, symmetric stretching and bending modes. The calculated vibrational frequencies for H_2O gas phase are: 3826, 3693, and 1589 cm^{-1}.

Metal	Site	E_a	α	D_{xy}	*h*	*d*O-metal	*z*	Vib. freq.
Al	*top*	−0.26	82	0.19	2.16	2.17	0.23	3570 3467 1530
	bridge	−0.10	102	0.05	3.10	3.36 3.46	0.07 −0.02	3763 3648 1581
	fcc	−0.10	94	0	3.37	3.74 3.76(2)	0	3795 3688 1588
	hcp	−0.09	93	0.07	3.35	3.70 3.74 3.77	0	3790 3682 1582
Rh	*top*	−0.35	92	0.14	2.32	2.33	0.07	3620 3501 1536
	bridge	−0.15	97	0.07	2.93	3.18 3.21	0.03 0	3676 3553 1552
	fcc	−0.13	90	0.03	3.20	3.53 3.56(2)	0	3725 3612 1565
	hcp	−0.13	91	0.09	3.18	3.50 3.55 3.58	0	3715 3591 1590

molecule also lies parallel to the surface plane, as shown in Table I. Cluster calculations[28] found adsorption energies for the *bridge* site of 0.34 eV and 0.18 eV (7.9 kcal/mol and 4.2 kcal/mol) for different cluster sizes (Al_{10} and Al_{17}, respectively). Such calculations did not find any structure with H_2O molecularly adsorbed at either three-fold sites on Al{111}. A repulsive water-surface interaction was found when studying the adsorption with the minimum clusters for these two sites (Al_4 and Al_7 for *hcp* and *fcc hollow* sites, respectively).

No other stable adsorption configuration was found at any of the four studied sites: *top*, *bridge*, *hcp,* and *fcc hollow*. The molecular plane is nearly parallel to the surface plane in every one of the studied sites in any of the studied surfaces (Al{111} and Rh{111}).

The column on the right of Table I shows that all the H_2O calculated vibrational frequencies undergo a downshift after adsorption from the gas phase values. On the Al surface the stretching modes are slightly more modified than on the Rh surface for the *top* configuration (241 cm^{-1} on Al, on average, against 199 cm^{-1} on Rh); whereas the bending mode is modified almost in the same quantity ($\approx$55 cm^{-1}) on both surfaces. For the *bridge* and *hollow* configurations, the vibrational frequencies are less modified on Al than on Rh. On the Al surface, the stretching vibrational modes are perturbated in the range 10–60 cm^{-1} from the gas phase; whereas the range is 80–150 cm^{-1} on Rh. The bending mode is slightly modified on both surfaces.

Calculations are performed for H_2O diffusion on the Al{111} and on the Rh{111} surfaces from the most stable *top* site along three different pathways: to the *bridge*, *fcc hollow,* and *hcp hollow* sites. Three different orientations of the molecular dipole are tested with respect to the investigated path: parallel, antiparallel, and perpendicular, with the molecular plane nearly parallel to the surface plane. Calculated MEPs show an absolute minimum for H_2O in the *top* configuration, regardless the orientation of the water dipole, as long as the molecular plane is nearly parallel to the surface plane. The vertical axis of Figures 2–4 is the energy relative to the adsorption energy of the water molecule on the *top* configuration of the corresponding substrate. The MEPs reveal maxima around the *fcc hollow*, *hcp hollow,* and *bridge* configurations. The right part of the MEPs of Figures 2–4 shows that the maxima are about 2 to 3.5 Å in the Reaction coordinate axis. As stated in Sec. II, the *climbing image nudged elastic band* method is used in this article. The energy data points are the energies of the images and are marked with dots along the MEPs. The image with the highest energy is *pushed* to the maximum of the MEP. Consequently, the third image (fourth energy point from the left) is *pushed up* to the maximum, the distance between the third image and the end point (*bridge* or *hollow* configuration) is shorter than the other distances in the reaction coordinate axis. The energy difference between the energy of the third image and the energy of the *bridge* or *hollow* configuration is smaller than

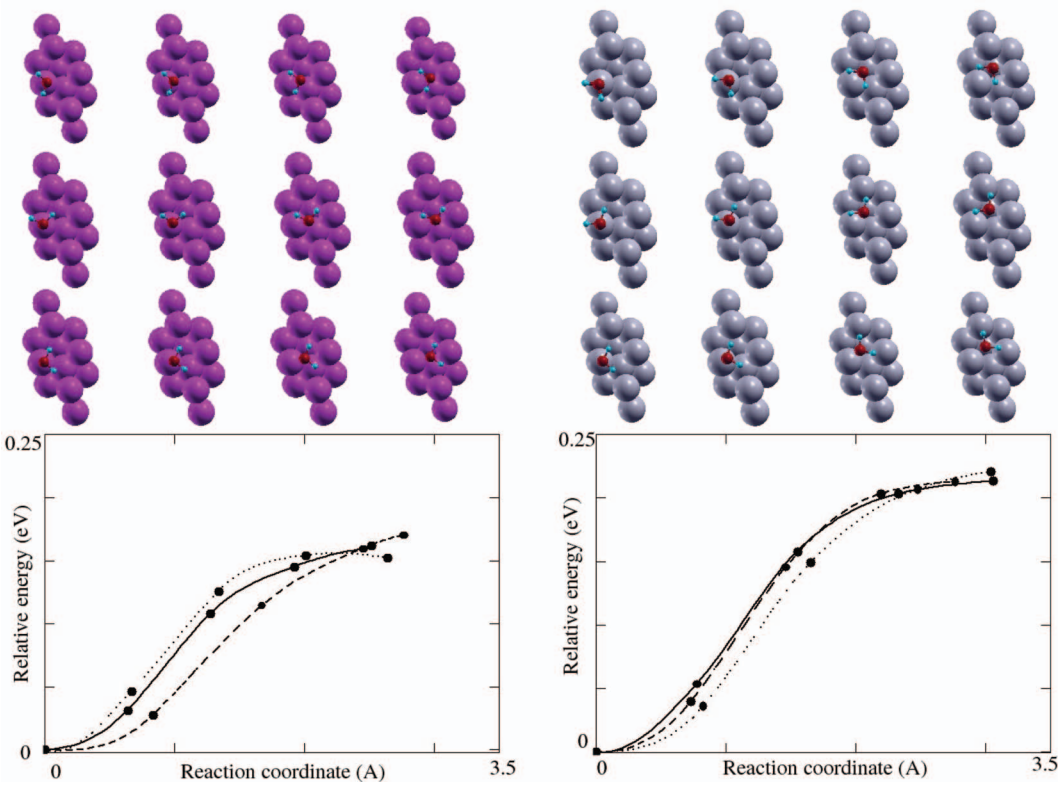

FIG. 2. (Bottom part): Calculated minimum energy pathways (MEPs) for three different orientations of the H_2O dipole relative to the *top-bridge* line on the Al{111} surface (left), and to the *top-fcc hollow* line on the Rh{111} surface (right). The plane of the water molecule is nearly parallel to the plane of the surface. The dots along the MEPs represent energy data points. The lines connecting the energy data points act as guide to the eye. Solid, dashed, and dotted lines stand for the parallel, perpendicular, and antiparallel orientations of the molecular dipole, respectively. (Upper part): Big, medium, and small spheres represent metal, oxygen, and hydrogen atoms, respectively. The representations are shown for some of the data points energy.

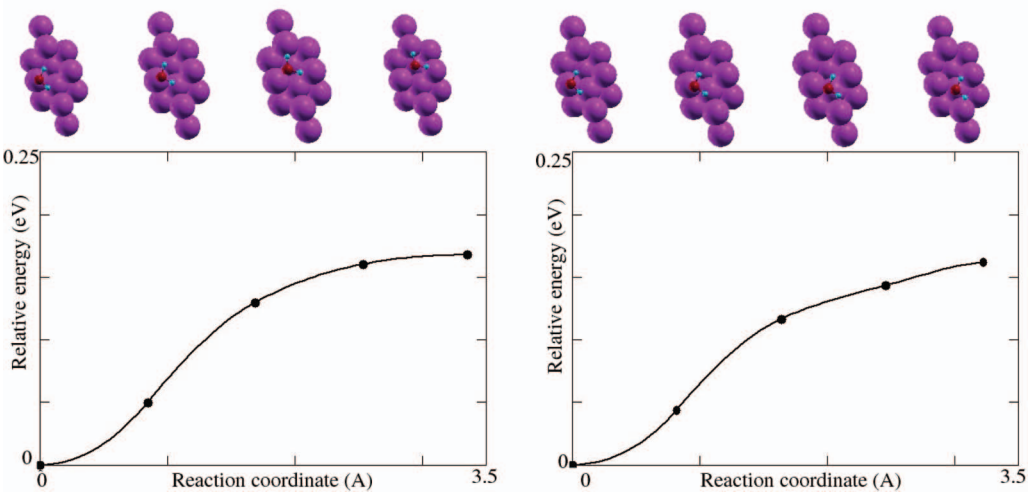

FIG. 3. (Bottom part): Calculated minimum energy pathways (MEPs) for H_2O on the Al{111} surface. The panels on the left and on the right show the MEPs between the *top-fcc hollow* configurations and the *top-hcp hollow* configurations, respectively. The plane of the water molecule is nearly parallel to the plane of the surface. The dots along the MEPs stand for energy data points. The lines connecting the energy data points serve as guide to the eye. Solid lines stand for the parallel orientation of the molecular dipole relative to the imaginary line between the *top* and the other high-symmetry configurations. (Upper part): Big, medium and small spheres represent metal, oxygen, and hydrogen atoms, respectively. The representations are shown for some of the data points energy.

0.02 eV for every MEP shown in Figures 2–4. This indicates a wide maximum is found in every MEP shown in the mentioned figures around the *bridge* and *hollow* sites.

Figures 2–4 also show that there are no local minima or local maxima between the global minimum and the global maximum in the depicted MEPs. The upper part of every MEP shows pictures of spheres or balls that represent the positions of the atoms for some configurations of the energy data points (not all the energy data points are represented).

The shape of all the MEPs resembles a sinelike or cosinelike function. This is in agreement with the universal assumption that the potential energy surface for the diffusion of an adsorbate species across a homogeneous surface is described as a cosinelike function with high-symmetry sites as the only stable configurations,[26] though it is known that this is not always the case. A different potential energy pathway shows the CO diffusion on the Pt{110} surface.[22]

The profiles shown in Figures 2–4 indicate that the activation energy for the H_2O diffusion from the *top* site to the next *top* site through any of the other three high-symmetry sites (following the corresponding MEP) is around the energy difference between the high-symmetry site and the *top* site configurations. According to the results shown in Table I, the activation energies are around 0.16 (−0.10−(−0.26)) and 0.2 (−0.15−(−0.35)) eV on Al and Rh, respectively, following the *top* → *bridge* MEP (see Figures 2–4). The low activation energy for diffusion shows the diffusion of water is a likely process on these metal surfaces. The theoretical results described in Figures 2–4 show that there is no clear preferred diffusion pathway for H_2O on the aforementioned metal

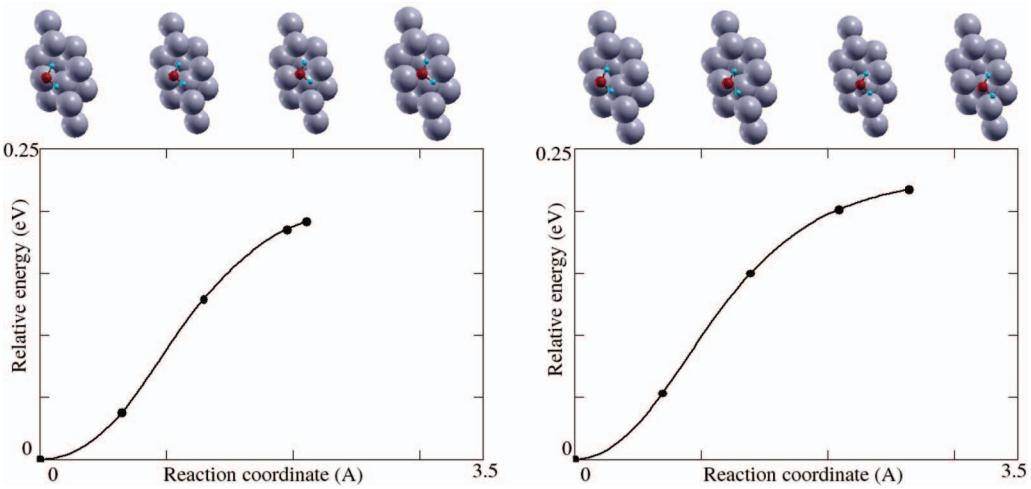

FIG. 4. (Bottom part): Calculated minimum energy pathways (MEPs) for H_2O on the Rh{111} surface. The panels on the left and on the right show the MEPs between the *top-bridge* configurations and the *top-hcp hollow* configurations, respectively. The plane of the water molecule is nearly parallel to the plane of the surface. The dots along the MEPs stand for energy data points. The lines connecting the energy data points serve as guide to the eye. Solid lines stand for the parallel orientation of the molecular dipole relative to the imaginary line between the *top* and the other high-symmetry configurations. (Upper part): Big, medium, and small spheres represent metal, oxygen, and hydrogen atoms, respectively. The representations are shown for some of the data points energy.

surfaces between *top* sites. This means that the diffusion of a H_2O molecule will be well described by a random walk process on these metal surfaces. On the same {111} surface but on different metal, this prediction is in line with experimental results on palladium.[6] In this experiment, a set of STM images show that the H_2O monomer spends most of the time on the *top* sites and the diffusion process is described by a random walk process at low temperature and low coverage.

Along each MEP, between ends, the orientation of the water dipole has little or no importance, as Figure 2 shows, as long as the molecular plane is nearly *parallel* to the surface plane. Rotation of the H_2O molecule around its dipole increases the energy up to instability. It has been shown that the interaction of the H_2O molecule with a {111} metal surface takes place via the $1b_1$ and $3a_1$ molecular orbitals (MOs).[16,19] The main attractive interaction is between the $1b_1$ MO, which is *perpendicular* to the molecular plane, and the surface wave functions. Rotation of the molecule around the molecular dipole will decrease this attractive interaction and so the stability.

IV. CONCLUSIONS

The potential energy surfaces of molecular water on the Al{111} and on the Rh{111} metal surfaces have been investigated using density functional theory and the climbing image nudged elastic band method. Similar landscapes of the potential energy surface were found for the interaction energy of H_2O with the Al{111} and Rh{111} metal surfaces at 0.25 ML coverage. Only one minimum was found where the water molecule is monocoordinated to the surface via the oxygen atom with its plane nearly parallel to the surface. The energy of the minimum, i.e., the water adsorption energy, is −0.26 eV in the case of Al and −0.35 eV in the case of Rh. The maxima are very close to the *bridge* and *hollow* configurations in the potential energy surface with energies of about −0.10 and −0.15 eV for Al and Rh, respectively; the molecular plane is nearly parallel to the surface plane. No local minima or local maxima were found along the investigated MEPs. The activation energy for water diffusion from the *top* site to the next *top* site, is estimated as 0.16 eV on Al and 0.20 eV on Rh, via the investigated MEPs. These small energy barriers indicate that the water diffusion on these surfaces is a likely process (at this coverage), even at low temperatures. This result is in agreement with experimental results on palladium at low coverage and low temperature.[6] Along the investigated minimum energy pathways, no strong preferential orientation of the water dipole was found on condition that the molecular plane is nearly parallel to the surface plane. Rotation of the H_2O molecule around the molecular dipole decreases the $1b_1$ MO interaction with the wavefunctions of the surface and causes instabilities.

ACKNOWLEDGMENTS

This work has been supported by Consejo de Investigaciones Científicas y Técnicas (CONICET). Many thanks to Professor Graeme Henkelman for his invaluable help with the NEB method.

[1] P. A. Thiel and T. E. Madey, Surf. Sci. Rep. **6–8**, 211 (1987).
[2] M. A. Henderson, Surf. Sci. Rep. **46**, 1–308 (2002).
[3] A. Verdaguer, G. M. Sacha, H. Bluhm, and M. Salmeron, Chem. Rev. **106**, 1478–1510 (2006).
[4] K. Morgenstern, T. Michely, and G. Comsa, Phys. Rev. Lett. **77**, 703 (1996).
[5] K. Morgenstern and J. Nieminen, Phys. Rev. Lett. **88**, 066102 (2002).
[6] T. Mitsui, M. K. Rose, E. Fomin, D. F. Ogletree, and M. Salmeron, Science **297**, 1850 (2002).
[7] M. Morgenstern and K. H. Rieder, J. Chem. Phys. **116**, 5746 (2002).
[8] K. Jacobi, B. Bedurftig, Y. Wang, and G. Ertl, Surf. Sci. **472**, 9 (2001).
[9] A. L. Glebov, A. P. Graham, and A. Menzel, Surf. Sci. **427**, 22 (1999).
[10] K. D. Gibson, M. Viste, and S. J. Sibener, J. Chem. Phys. **112**, 9582 (2000).
[11] A. Michaelides and P. Hu, J. Chem. Phys. **114**, 513 (2001).
[12] A. Michaelides and P. Hu, J. Am. Chem. Soc. **114**, 2523 (2001).
[13] P. J. Feibelman, Phys. Rev. Lett. **90**, 186103 (2000).
[14] P. J. Feibelman, Science **295**, 99 (2002).
[15] S. Meng, L. F. Xu, E. G. Wang, and S. Gao, Phys. Rev. Lett. **89**, 176104 (2002).
[16] A. Michaelides, V. A. Ranea, P. L. de Andrés, and D. A. King, Phys. Rev. Lett. **90**, 216102 (2003).
[17] A. Michaelides, V. A. Ranea, P. L. de Andrés, and D. A. King, Phys. Rev. B **69**, 075409 (2004).
[18] V. A. Ranea, A. Michaelides, R. Ramírez, P. L. de Andrés, J. A. Vergés, and D. A. King, Phys. Rev. Lett. **92**, 136104 (2004).
[19] V. A. Ranea, A. Michaelides, R. Ramírez, J. A. Vergés, P. L. de Andrés, and D. A. King, Phys. Rev. B **69**, 205411 (2004).
[20] G. Greeley, J. K. Norskov, and M. Mavrikakis, Annu. Rev. Phys. Chem. **53**, 319 (2002).
[21] R. A. van Saten and M. Neurock, Catal. Rev. - Sci. Eng. **37**, 557 (1995).
[22] Q. Ge and D. A. King, J. Chem. Phys. **111**, 9461 (1999).
[23] Q. Ge and D. A. King, J. Chem. Phys. **114**, 1053–1054 (2001).
[24] J. Kua, W. Ho, and W. A. Goddard III, J. Chem. Phys. **115**, 5620 (2001).
[25] X. Sha and B. Jacson, Chem. Phys. Lett. **357**, 389 (2002).
[26] D. A. King, J. Vac. Sci. Technol. **17**, 241 (1980).
[27] F. Hofmann and J. P. Toennies, Chem. Rev. **96**, 1307 (1996).
[28] S. Jin and J. D. Head, Surf. Sci. **318**, 204 (1994).
[29] P. Hohenberg and W. Kohn, Phys. Rev. **136**, B864 (1964).
[30] W. Kohn and L. J. Sham, Phys. Rev. A **140**, 1133 (1965).
[31] G. Kresse and J. Hafner, Phys. Rev. B **49**, 14251 (1994).
[32] G. Kresse and J. Furthmuller, Phys. Rev. B **54**, 11169–11186 (1996).
[33] P. Blöchl, Phys. Rev. B **50**, 17953–17979 (1994).
[34] G. Kresse and J. Joubert, Phys. Rev. B **59**, 1758 (1999).
[35] J. P. Perdew, J. A. Chevary, S. H. Vosko, K. A. Jackson, M. R. Pederson, D. J. Singh, and C. Fiolhais, Phys. Rev. B **46**, 6671 (1992).
[36] H. Jónsson, G. Mills, and K. Jacobsen, *Classical and Quantum Dynamics in Condensed Phase Simulations*, edited by B. Berne, G. Ciccotti, and D. Cocker (World Scientific, River Edge, NJ, 1998), pp. 389–405.
[37] G. Henkelman, B. P. Uberuaga, and H. Jónsson, J. Chem. Phys. **113**, 9901–9904 (2000).
[38] H. J. Monkhorst and J. D. Pack, Phys. Rev. B **13**, 5188 (1976).
[39] R. W. G. Wyckoff, *Crystal Structures*, 2nd ed. (Interscience, New York, 1965).